The hadronic contribution to the running of the electromagnetic coupling and the electroweak mixing angle (Part I)

Marco Cè Antoine Gérardin Georg von Hippel Harvey B. Meyer
Kohtaroh Miura Konstantin Ottnad Andreas Risch
Teseo San José Jonas Wilhelm Hartmut Wittig

Accepted for publication by JHEP
arXiv:2203.08676

$\alpha(M_Z^2)$ and $\sin^2\theta_W(Q^2 \ll M_Z^2)$

Two important quantities for precision tests of the SM

$$\alpha(M_Z^2) = 1/127.951(9)$$ [Zyla et al. 2020]

$$\sin^2\theta_W(0.025\,\text{GeV}^2) = 0.2383(11)$$ [Androić et al. 2018]

Upcoming experiments will improve precision → Need more precise theoretical determination
Main source of uncertainty: Leading hadronic contribution
Standard theoretical approach:

$$\underbrace{\frac{\sigma(e^+e^- \to \text{hadrons})}{\sigma(e^+e^- \to \mu^+\mu^-)}}_{\text{time-like experiments}} + \begin{cases} \text{perturbation theory} \to (\Delta\alpha)_{\text{had}}(M_Z^2) \\ \text{flavour separation} \to (\Delta\sin^2\theta_W)_{\text{had}}(Q^2 \ll M_Z^2) \end{cases}$$

A lattice determination has several advantages:

- ➔ Replace experimental data with *ab initio* calculation
- ➔ Exact flavour separation

I explain how to obtain $(\Delta\alpha)_{\text{had}}(-Q^2)$ and $(\Delta\sin^2\theta_W)_{\text{had}}(-Q^2)$ at $Q^2 \sim 1\,\text{GeV}^2$
[H. Wittig, TUE 18:10] explains how to connect $\alpha(M_Z^2)$ and $\alpha(-Q^2)$

Computational setup [Bruno et al. 2015; Bruno, Korzec, and Schaefer 2017]

$N_f = 2 + 1$ $\mathcal{O}(a)$-improved Wilson action

Tree-level improved Lüscher-Weisz action

Periodic/open temporal boundary conditions

Chiral trajectory $M_\pi^2/2 + M_K^2 \approx$ const

Pion masses $130\,\text{MeV} < M_\pi < 420\,\text{MeV}$

$a = 0.05\,\text{fm},\ 0.064\,\text{fm},\ 0.076\,\text{fm},\ 0.086\,\text{fm}$

Volumes $M_\pi L > 4$

Local and conserved discretisations

Scale setting [Bruno, Korzec, and Schaefer 2017]

$$\sqrt{8t_0} = 0.415\ (4)\ (2)\ \text{fm}.$$

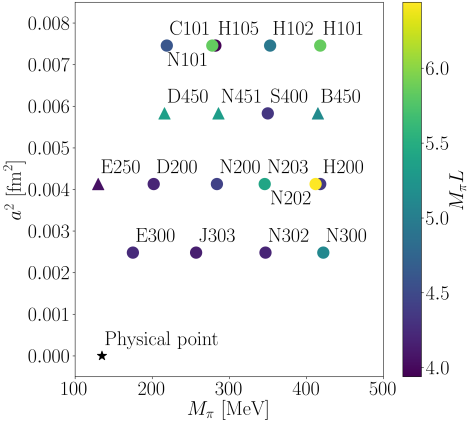

Time-momentum representation [Bernecker and H. B. Meyer 2011; Francis et al. 2013]

As a function of the momentum exchanged $Q^2 > 0$,

$$\alpha(-Q^2) = \alpha/(1 - \Delta\alpha(-Q^2)), \qquad \sin^2\theta_W(-Q^2) = \sin^2\theta_W\left(1 + \Delta\sin^2\theta_W(-Q^2)\right)$$

The leading hadronic contributions are related to two subtracted vacuum polarisations:

$$(\Delta\alpha)_{\text{had}}(-Q^2) = 4\pi\alpha\,\bar{\Pi}^{\gamma\gamma}(-Q^2), \qquad (\Delta\sin^2\theta_W)_{\text{had}}(-Q^2) = -4\pi\alpha/\sin^2\theta_W\,\bar{\Pi}^{Z\gamma}(-Q^2)$$

Use the time-momentum representation to express the subtracted vacuum polarisation

$$\bar{\Pi}^{Z(\gamma)\gamma}(-Q^2) = \int_0^\infty \mathrm{d}t\; G^{Z(\gamma)\gamma}(t)K(t,Q^2), \quad G^{Z(\gamma)\gamma}(t) = -\frac{1}{3}\sum_{j=1,2,3}\int \mathrm{d}\vec{x}\,\left\langle \bar{V}_j^{Z(\gamma)}(x)V_j^{\gamma}(0)\right\rangle_{\text{QCD}}$$

$$V_\mu^\gamma = V_\mu^3 + 1/\sqrt{3}V_\mu^8 + 4/9V_\mu^c \qquad V_\mu^Z = (1/2 - \sin^2\theta_W)V_\mu^\gamma - 1/6V_\mu^0 - 1/12V_\mu^c$$

$$V_\mu^{3,8,0} = 1/2\bar{q}\gamma_\mu\lambda^{3,8,0}q \qquad V_\mu^c = \bar{c}\gamma_\mu c$$

$\lambda^3 = \text{diag}(1,-1,0)$, $\lambda^8 = \text{diag}(1,1,-2)$, $\lambda^0 = \text{diag}(1,1,1)$ act in flavour space. $q = (u,d,s)$

Bounding method [Borsanyi et al. 2018]

$$0 \leq G(t_{\rm cut})e^{-M_{\rm eff}(t)(t-t_{\rm cut})} \leq G(t) \leq G(t_{\rm cut})e^{-E_0(t-t_{\rm cut})}, \qquad t \geq t_{\rm cut},$$

where

$M_{\rm eff}(t) = \log\left[G(t)/G(t+a)\right]$ is the effective mass.

E_0 is the ground state,

Example at physical M_π:

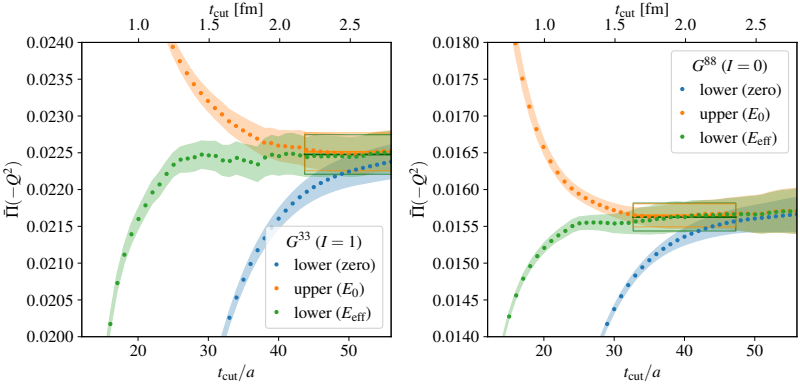

Finite-size effects

The infinite-volume correlator is obtained from the corrected finite-volume case,

$$G(t,\infty) = G(t,L) + \Delta G(t,L),$$

$$\Delta G(t,L) = G_{\text{model}}(t,\infty) - G_{\text{model}}(t,L).$$

We estimate the correction $\Delta G(t,L)$ via the Meyer-Lellouch-Lüscher method,

$$G_{\text{model}}(t,\infty) = \int_{2M_\pi}^{\infty} \mathrm{d}\omega\ \omega^2 \rho(\omega^2) e^{-\omega t},$$

$$G_{\text{model}}(t,L) \overset{t\to\infty}{=} \sum_n |A_n|^2 e^{-t\omega_n},$$

where both $\rho(\omega^2)$ and $|A_n|$ can be related to the time-like pion form factor $F_\pi(\omega)$.

At $M_\pi = 280\,\text{MeV}$, $M_\pi L = 4$,

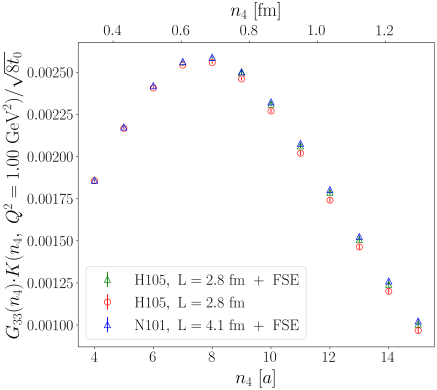

$$\sum_t \Delta G^{33}(t,L)\, K(t,Q^2) = \Delta\bar{\Pi}^{33}(L = 2.8\,\text{fm}, Q^2 = 1\,\text{GeV}^2) = 57 \times 10^{-5}\ (2\%)$$

[Meyer 2011; Francis et al. 2013; Della Morte et al. 2017; Lellouch and Luscher 2001]

Finite-size effects

The infinite-volume correlator is obtained from the corrected finite-volume case,

$$G(t,\infty) = G(t,L) + \Delta G(t,L),$$

$$\Delta G(t,L) = G_{\text{model}}(t,\infty) - G_{\text{model}}(t,L).$$

We estimate the correction $\Delta G(t,L)$ via the Meyer-Lellouch-Lüscher method,

$$G_{\text{model}}(t,\infty) = \int_{2M_\pi}^{\infty} \mathrm{d}\omega\ \omega^2 \rho(\omega^2) e^{-\omega t},$$

$$G_{\text{model}}(t,L) \overset{t\to\infty}{=} \sum_n |A_n|^2 e^{-t\omega_n},$$

where both $\rho(\omega^2)$ and $|A_n|$ can be related to the time-like pion form factor $F_\pi(\omega)$.
Or via the Hansen-Patella method, which uses a relativistic effective theory of pions with local interactions.
[Hansen and Patella 2020; Hansen and Patella 2019]

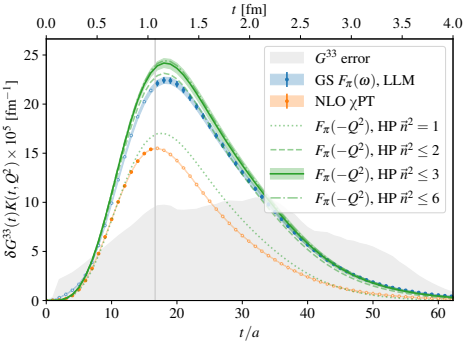

Extrapolation at $Q^2 = 1\,\text{GeV}^2$

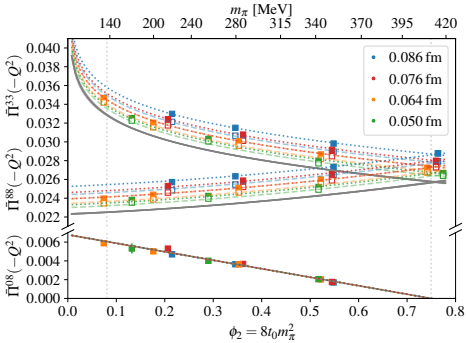

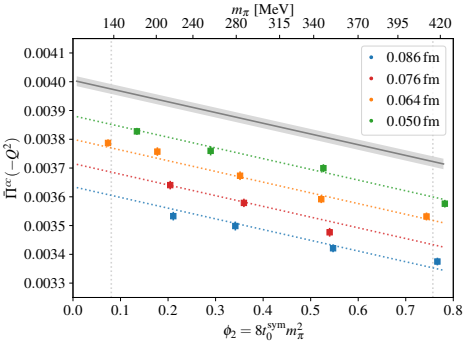

Scale setting — charm-quark loops — Total

$$(\Delta\alpha)_{\text{had}}(-1\,\text{GeV}^2) \times 10^6 = 3864\ (17)\ (8)\ (22)\ (4)\ (12)\ [32,\ 0.8]$$

Statistical — Extrapolation — Isospin breaking — Percentage

$$(\Delta \sin^2\theta_W)_{\text{had}}(-1\,\text{GeV}^2) \times 10^6 = -3927\ (19)\ (5)\ (32)\ (4)\ (13)\ [40,\ 1.0]$$

Scale-setting uncertainty

Dominant uncertainty for $0 < Q^2 \lesssim 3\,\mathrm{GeV}^2$

Although $\bar{\Pi}$ is dimensionless, the scale enters indirectly through

- The virtuality $8t_0 Q^2$ in the kernel $K(t, Q^2)$ of the TMR.
- The physical point definition ϕ_2^{phy}, ϕ_4^{phy}.

Using linear error propagation, the relative error of $\bar{\Pi}$ is

$$\frac{\Delta\bar{\Pi}}{\bar{\Pi}} \approx \left| \frac{2l_0^2 Q^2}{\bar{\Pi}} \frac{\partial\bar{\Pi}}{\partial l_0^2 Q^2} + \frac{2\phi_2^{\mathrm{phy}}}{\bar{\Pi}} \frac{\partial\bar{\Pi}}{\partial\phi_2^{\mathrm{phy}}} + \frac{2\phi_4^{\mathrm{phy}}}{\bar{\Pi}} \frac{\partial\bar{\Pi}}{\partial\phi_4^{\mathrm{phy}}} \right| \frac{\Delta l_0}{l_0}$$

The first term is positive, and varies with Q^2
The second and third terms are negative
$\Delta\bar{\Pi}/\bar{\Pi} \sim 0$ in some cases

$\rightarrow$ We use bootstrap sampling instead

Scale setting: $l_0 \equiv \sqrt{8t_0} = 0.415\ (4)\ (2)$ fm [Bruno, Korzec, and Schaefer 2017]

Improved determination in progress [A. Segner, THU 10:20]

Missing quark contributions

The charm-quark contribution is determined from the quark-connected component alone. Therefore, there are two missing effects:

- ➔ Valence charm-quark loops

  [Borsanyi et al. 2018] reports this contribution to be $< 1\%$ of the u, d, s quark-disconnected contribution to $a_\mu^{\mathrm{HVP,LO}}$ $\rightarrow$ 0.1‰ effect we neglect

- ➔ Sea charm-quark loops

  To estimate the effect of quenching, we employ a phenomenological estimate,

  Split $\bar{\Pi}$ into two parts,

$$\bar{\Pi}(-Q_0^2) = \underbrace{\left[\bar{\Pi}(-Q_0^2) - \bar{\Pi}(-1\,\mathrm{GeV}^2)\right]}_{①} + \underbrace{\bar{\Pi}(-1\,\mathrm{GeV}^2)}_{②}$$

① Charm sea-quark effects appear at $\mathcal{O}\left(\alpha_s^2\right)$ in perturbation theory $\rightarrow$ negligible

② D^+D^-, $D^0\bar{D}^0$, $D_s^+D_s^-$ contribute to the (u,d,s) vector correlators.
Using scalar-QED $\rightarrow$ 3‰ effect added to error budget

The bottom-quark contribution is determined by [Colquhoun et al. 2015] $\rightarrow$ maximum 3‰ effect added to error budget to compare with phenomenology

Isospin breaking effects [Risch and Wittig 2022; Risch 2021; Risch and Wittig 2019]

Evaluate quark-connected $\bar{\Pi}$ in QCD + QED at $M_\pi \sim 220\,\text{MeV}$ → Estimate relative size of isospin breaking effects → Add to error budget

- → Non-compact QED_L-action for IR regularisation, Coulomb gauge [Hayakawa and Uno 2008]
- → Same boundary conditions for the photon and gluon fields
- → Reweighting and leading perturbative expansion in $\Delta\epsilon = \epsilon - \epsilon^{(0)}$ around $\epsilon^{(0)}$, where

  QCD + QED parametrised by $\epsilon = \left(M_u, M_d, M_s, \beta, e^2\right)$

  QCD_iso parametrised by $\epsilon^{(0)} = (M_{ud}^{(0)}, M_{ud}^{(0)}, M_s^{(0)}, \beta^{(0)}, 0)$

  [Divitiis et al. 2012; Divitiis et al. 2013]
- → Neglect IB effects in the scale
- → Renormalisation scheme: Match QCD + QED and QCD_iso using

$$M_{\pi^0}^2 \propto M_u + M_d$$

$$M_{K^+}^2 - M_{K^0}^2 - M_{\pi^+}^2 + M_{\pi^0}^2 \propto M_u - M_d$$

$$M_{K^+}^2 + M_{K^0}^2 - M_{\pi^+}^2 \propto M_s$$

Running of $(\Delta\alpha)_{\text{had}}$ and $(\Delta \sin^2\theta_W)_{\text{had}}$

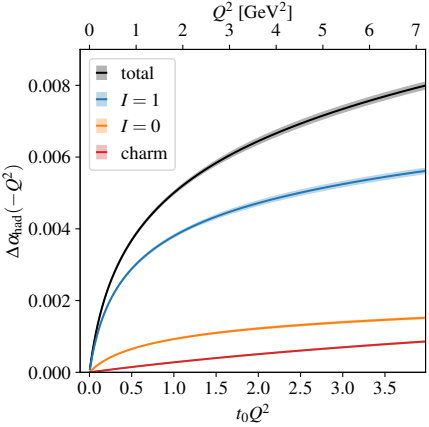

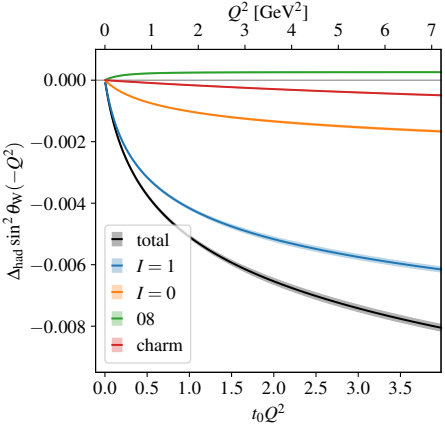

Padé approximants in the range $0 \leq Q^2 \leq 7\,\text{GeV}^2$

Sample $\bar{\Pi}$ in a wide range of Q^2, and fit all data-points to a multi-point Padé Ansatz [Aubin et al. 2012],

$$\bar{\Pi}(-Q^2) \approx \frac{\sum_{j=0}^{M} a_j Q^{2j}}{1 + \sum_{k=1}^{N} b_k Q^{2k}}$$

Then, the running couplings in the range $0 \leq Q^2 \leq 7\,\text{GeV}^2$ are

$$(\Delta\alpha)_{\text{had}}(-Q^2) = 4\pi\alpha\,\frac{0.1094(23)\,x + 0.093(15)\,x^2 + 0.0039(6)\,x^3}{1 + 2.85(22)\,x + 1.03(19)\,x^2 + 0.0166(12)\,x^3}$$

$$(\Delta \sin^2\theta_W)_{\text{had}}(-Q^2) = -\frac{4\pi\alpha}{\sin^2\theta_W}\,\frac{0.022\,63(6)\,x + 0.025(5)\,x^2 + 0.000\,89(34)\,x^3}{1 + 2.94(29)\,x + 1.12(27)\,x^2 + 0.015(8)\,x^3}$$

with $x = Q^2/\text{GeV}^2$, $4\pi\alpha = 0.091701236853(14)$ and $\sin^2\theta_W = 0.23857(5)$ [Zyla et al. 2020].

To reproduce the error bands, we give the correlation matrix of the coefficients.

Comparison with other lattice and phenomenological estimates

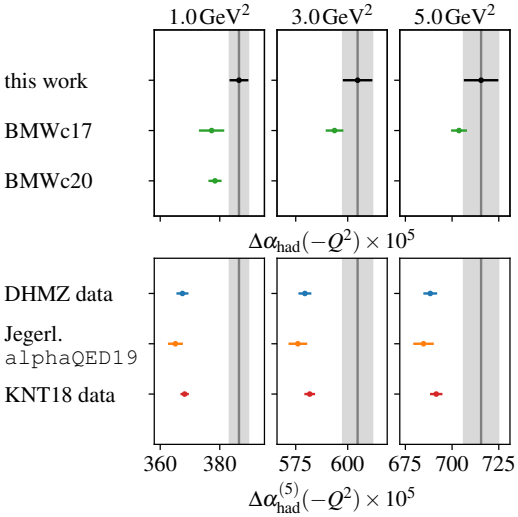

1-2 sigma disagreement between this work and [Borsanyi et al. 2018; Borsanyi et al. 2021]

3-6 sigma disagreement between our results and [Keshavarzi, Nomura, and Teubner 2020; Davier et al. 2020; Jegerlehner 2020]

Summary

- → Computation of $(\Delta\alpha)_{\text{had}}$ and $(\Delta \sin^2\theta_W)_{\text{had}}$ in the space-like interval $0 \leq Q^2 \leq 7\,\text{GeV}^2$
- → Estimate of all error sources (2% for $Q^2 < 1\,\text{GeV}^2$, 1% for $Q^2 > 1\,\text{GeV}^2$)
- → Results in closed form using Padé approximants and correlation matrices
- → Significant tension with the data-driven method

Ongoing and related work

- → Full calculation of isospin breaking effects [Risch and Wittig 2022; Risch 2021]
- → Improved scale setting [A. Segner, THU 10:20]
- → Isovector $\pi\pi$-scattering at physical M_π [S. Paul, FRI 15:10]
- → Intermediate window observable for $a_\mu^{\text{HVP,LO}}$ [S. Kuberski, TUE 17:10]

Up next,

- → Connection between $(\Delta\alpha)_{\text{had}}(-Q^2)$ and $(\Delta\alpha)_{\text{had}}(M_Z^2)$ [H. Wittig, TUE 18:10]

CLS $N_f = 2 + 1$ ensembles [Bruno et al. 2015; Bruno, Korzec, and Schaefer 2017]

	T/a	L/a	$t_0^{\rm sym}/a^2$	a [fm]	L [fm]	M_π, M_K [MeV]		$M_\pi L$	# cnfg (con., dis., charm)		
H101	96	32	2.86	0.08636	2.8	418		5.9	2000	-	1000
H102	96	32			2.8	353	438	4.9	1900	1900	975
H105*	96	32			2.8	281	463	3.9	1000	1000	500
N101	128	48			4.1	279	461	5.9	1155	1155	345
C101	96	48			4.1	219	470	4.6	2000	2000	400
B450	64	32	3.659	0.07634	2.4	414		5.1	1600	-	800
S400	128	32			2.4	351	441	4.3	1720	1720	800
N451	128	48			3.7	286	460	5.3	1000	1000	200
D450	128	64			4.9	216	475	5.3	500	500	300
H200*	96	32	5.164	0.06426	2.1	418		4.4	1980	-	480
N202	128	48			3.1	411		6.4	875	-	420
N203	128	48			3.1	345	442	5.4	1500	1500	700
N200	128	48			3.1	283	462	4.4	1695	1695	390
D200	128	64			4.1	201	480	4.2	2000	1000	500
E250	192	96			6.2	129	489	4.1	485	485	65
N300	128	48	8.595	0.04981	2.4	422		5.1	1680	-	480
N302	128	48			2.4	346	451	4.2	2190	1080	480
J303	192	64			3.2	257	474	4.2	1040	1040	100
E300	192	96			4.8	175	491	4.2	600	300	100

* only used in the estimation of finite-size effects.

The Γ method vs jackknife binning [Wolff 2004; Bruno et al. 2015]

Measurements are taken every 4 MDU.
Runs with the same trajectory length should show Langevin scaling, $\bar{\bar{\tau}}_{\bar{\Pi},\mathrm{int}} \propto a^{-2}$. OBC are taking to alleviate the increase in autocorrelations towards the The error estimate using the Γ method includes autocorrelations explicitly,

$$\left(\Delta\bar{\bar{F}}\right)^2 = 2\bar{\bar{\tau}}_{F,\mathrm{int}}\left(\Delta_0\bar{\bar{F}}\right)^2, \qquad \left(\Delta_{\mathrm{jack}}\bar{F}\right)^2 = \frac{N_B-1}{N_B}\sum_{k=1}^{N_B}\left(f(c_\alpha^k)-\bar{F}\right)^2.$$

Both methods minimize the total error of the error to find the correct uncertainty,

$$\frac{\Delta_{\mathrm{total}}\left(\Delta\bar{\bar{F}}\right)}{\Delta\bar{\bar{F}}} \approx \frac{1}{2}\min_w\left(e^{-w/\tau_{F,\mathbf{D}}}+2\sqrt{\frac{w}{N}}\right), \qquad \frac{\Delta_{\mathrm{total}}\left(\Delta_{\mathrm{jack}}\bar{F}\right)}{\Delta_{\mathrm{jack}}\bar{F}} \approx \frac{1}{2}\min_B\left(\frac{\tau_{F,\mathrm{D}}}{B}+\sqrt{\frac{2B}{N}}\right).$$

The systematic error of the error is different,

$$\frac{\Delta_{\mathrm{sys}}\left(\Delta\bar{\bar{F}}\right)}{\Delta_{\mathrm{sta}}\left(\Delta\bar{\bar{F}}\right)} \approx \frac{1}{\log\left(N/\tau_{F,\mathrm{D}}\right)}, \qquad \frac{\Delta_{\mathrm{sys}}\left(\Delta_{\mathrm{jack}}\bar{F}\right)}{\Delta_{\mathrm{sta}}\left(\Delta_{\mathrm{jack}}\bar{F}\right)} = \frac{1}{2}.$$

The systematic error of the error for the Γ method vanishes with increasing statistics.

Time-momentum representation [Bernecker and H. B. Meyer 2011; Francis et al. 2013]

$$K(t, Q^2) = t^2 - \frac{4}{Q^2} \sin^2\left(\frac{Qt}{2}\right)$$

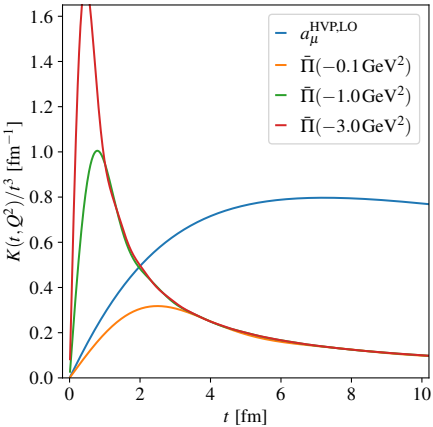

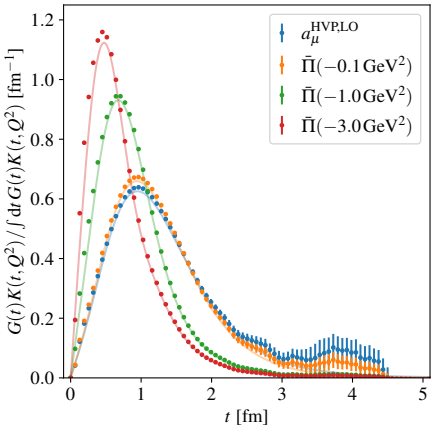

Autocorrelation analysis [Wolff 2004]

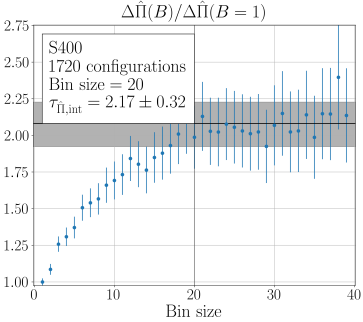

Ensemble S400, with $M_\pi = 351$ MeV

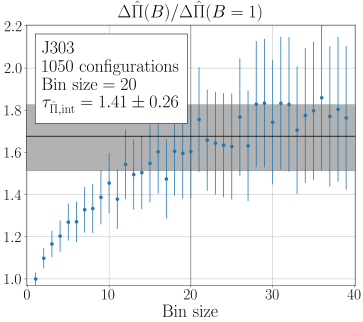

Ensemble J303, with $M_\pi = 257$ MeV

The vertical line shows the estimated optimal bin size B, and the horizontal band shows

$$\Delta\bar{\Pi}(B)/\Delta\bar{\Pi}(1) = \sqrt{2\tau_{\bar{\Pi},\mathrm{int}}} = \mathrm{const},$$

which is the expected uncertainty increase when taking into account autocorrelations.

Autocorrelation analysis

CLS	aM_π	Bin size	$\tau_{\bar{\Pi},\mathrm{int}}$
H101	0.1830 (5)	25	1.70 (26)
H102	0.1546 (5)	25	1.73 (27)
H105	0.1234 (13)	20	1.32 (27)
N101	0.1222 (5)	15	0.79 (11)
C101	0.0960 (6)	20	0.79 (10)
B450	0.1605 (4)	25	1.45 (24)
S400	0.1358 (4)	20	2.17 (32)
N451	0.1108 (3)	10	0.73 (10)
D450	0.0836 (4)	5	0.55 (7)
H200	0.1363 (5)	30	1.20 (19)
N202	0.1342 (3)	35	1.86 (45)
N203	0.1124 (2)	20	1.15 (17)
N200	0.0922 (3)	15	0.77 (10)
D200	0.0655 (3)	10	0.58 (6)
E250	0.0422 (2)	5	0.47 (4)
N300	0.1067 (3)	40	3.36 (67)
N302	0.0875 (3)	30	2.07 (33)
J303	0.0649 (2)	20	1.41 (26)
E300	0.0442 (1)	20	1.07 (22)

The pion masses were obtained by the Mainz group using an implementation of the PhD thesis [Risch 2021]. B and $\tau_{\bar{\Pi},\mathrm{int}}$ are computed using the *Python* code [De Palma et al. 2019].

Bounding method's spectra

Label	aM_π	$aE_{\pi\pi}$	$aE_{\pi\pi\pi}$ [1]	$aM_{\rho,GS}$	aM_ρ [2]	aM_ρ
H101	0.1836(5)	0.5376(7)	0.8704(9)	0.375(2)	-	0.375(2)
H102	0.1546(6)	0.4998(7)	0.8176(10)	0.358(3)	-	0.358(3)
H105	0.1235(13)	0.4639(14)	0.7679(19)	0.338(11)	-	0.338(11)
N101	0.1224(5)	0.3584(6)	0.5803(9)	0.340(4)	-	0.340(4)
C101	0.0962(6)	0.3248(8)	0.5335(11)	0.334(4)	0.326(3)	0.326(3)
B450	0.1611(4)	0.5079(6)	0.8290(8)	0.337(1)	-	0.337(1)
S400	0.1359(4)	0.4776(5)	0.7868(7)	0.312(4)	-	0.312(4)
N401	0.1100(6)	0.3419(8)	0.5572(11)	0.303(6)	0.299(2)	0.299(2)
N451	0.1109(3)	0.3431(4)	0.5589(5)	0.302(4)	-	0.302(4)
D450	0.0836(4)	0.2579(5)	0.4200(7)	0.303(8)	-	0.303(8)
H200	0.1363(5)	0.4781(5)	0.7874(8)	0.286(3)	-	0.286(3)
N202	0.1342(3)	0.3750(4)	0.6036(6)	0.280(3)	-	0.280(3)
N203	0.1127(2)	0.3454(3)	0.5621(4)	0.269(2)	0.268(1)	0.268(1)
N200	0.0923(3)	0.3204(3)	0.5273(4)	0.260(4)	0.252(2)	0.252(2)
D200	0.0651(3)	0.2357(3)	0.3890(4)	0.256(3)	0.250(2)	0.250(2)
E250	0.0422(3)	0.1557(3)	0.2574(4)	0.242(5)	0.251(4)	0.251(4)
N300	0.1062(2)	0.3371(3)	0.5505(4)	0.222(3)	-	0.222(3)
N302	0.0872(3)	0.3146(4)	0.5193(5)	0.216(3)	-	0.216(3)
J303	0.0648(2)	0.2353(2)	0.3885(3)	0.194(3)	0.200(2)	0.200(2)
E300	0.0437(2)	0.1574(2)	0.2597(2)	0.198(2)	-	0.198(2)

[1] Hansen, Romero-López, and Sharpe 2020.
[2] Andersen et al. 2019.

$\bar{\Pi}_{33}$, $\bar{\Pi}_{88}$, $\bar{\Pi}_{cc}$ and $\bar{\Pi}_{08}$ at a subset of virtualities

Q^2 [GeV^2]	$t_0 Q^2$	$\bar{\Pi}^{33}$	$\bar{\Pi}^{88}$
0.1	0.0553	0.007 64 (9) (8) (4)(0)[13]	0.004 06 (4)(0) (4)(0) [6]
0.4	0.2212	0.020 61 (15)(11)(10)(1)[21]	0.012 59 (8)(1)(11)(1)[14]
1.0	0.553	0.032 87 (17)(10)(21)(3)[29]	0.022 51 (9)(3)(19)(3)[21]
2.0	1.106	0.0429 (2) (1) (3)(1) [4]	0.031 69 (17)(5)(27)(5)[33]
3.0	1.659	0.0488 (5) (0) (4)(1) [6]	0.0374 (5)(1) (3)(1) [6]
4.0	2.212	0.0529 (6) (0) (4)(1) [7]	0.0414 (6)(1) (4)(1) [7]
5.0	2.764	0.0560 (6) (0) (5)(1) [8]	0.0445 (6)(1) (4)(1) [8]
Q^2 [GeV^2]	$t_0 Q^2$	$\bar{\Pi}^{08}$	$\bar{\Pi}^{cc}$
0.1	0.0553	0.001 75 (4)(0) (7)(0) [8]	0.000 421 (2)(1) (9)(–) [9]
0.4	0.2212	0.004 40 (7)(0)(14)(0)[15]	0.001 652 (7)(2)(33)(–)[34]
1.0	0.553	0.006 06 (8)(0)(15)(0)[17]	0.003 97 (2)(1) (8)(–) [8]
2.0	1.106	0.006 72 (8)(0)(15)(0)[17]	0.007 49 (3)(1)(14)(–)[14]
3.0	1.659	0.006 90 (8)(0)(15)(0)[17]	0.010 64 (4)(1)(19)(–)[19]
4.0	2.212	0.006 98 (8)(0)(15)(1)[17]	0.013 48 (5)(2)(23)(–)[24]
5.0	2.764	0.007 01 (8)(0)(15)(1)[17]	0.016 08 (6)(2)(26)(–)[27]

Uncertainties from left to right: statistical, fit, scale setting, charm loops and total

$(\Delta\alpha)_{\text{had}}$ and $(\Delta \sin^2\theta_W)_{\text{had}}$ at a subset of virtualities

Q^2 [GeV^2]	$t_0 Q^2$	$(\Delta\alpha)_{\text{had}}$	$(\Delta \sin^2\theta_W)_{\text{had}}$
0.1	0.0553	0.000 842 (9) (7) (4)(0) (2)[13]	−0.000 849 (10) (8) (5)(0)(1)[14]
0.4	0.2212	0.002 342 (15)(10)(12)(1) (7)[23]	−0.002 368 (17)(11)(18)(2)(3)[27]
1.0	0.553	0.003 864 (17) (8)(22)(4)(12)[32]	−0.003 93 (2) (1) (3)(0)(1) [4]
2.0	1.106	0.005 21 (2) (0) (3)(1) (2) [4]	−0.005 30 (3) (0) (4)(1)(1) [5]
3.0	1.659	0.006 05 (6) (0) (4)(1) (2) [7]	−0.006 14 (6) (0) (5)(1)(1) [8]
4.0	2.212	0.006 66 (7) (0) (4)(1) (2) [9]	−0.006 76 (8) (0) (6)(1)(1)[10]
5.0	2.764	0.007 16 (8) (0) (5)(2) (2) [9]	−0.007 24 (8) (0) (6)(2)(1)[10]
6.0	3.317	0.007 57 (8) (0) (5)(2) (2) [9]	−0.007 64 (8) (0) (6)(2)(1)[11]
7.0	3.87	0.007 93 (8) (0) (4)(2) (2) [9]	−0.007 99 (8) (0) (6)(2)(1)[11]

Uncertainties from left to right: statistical, fit, scale-setting, charm loops, isospin-breaking effects, and total

Extrapolation to the physical point

Extrapolate to the isospin-symmetric physical point on the dimensionless variables

[Bruno, Korzec, and Schaefer 2017; Zyla et al. 2020; Blum et al. 2021]

$$a^2/8t_0^{\rm sym} \to 0$$

$$\phi_2 = 8t_0 M_\pi^2 \to \phi_2^{\rm phy} = 0.0806(17)$$

$$\phi_4 = 8t_0(M_\pi^2/2 + M_k^2) \to \phi_4^{\rm phy} = 1.124(24)$$

Fit models

$$\bar{\Pi}^{\rm charm}(a^2/8t_0^{\rm sym}, \phi_2) = \bar{\Pi}^{\rm cc,sym} + \delta_2^d\left(a^2/8t_0^{\rm sym}\right) + \gamma_1^{cc}\left(\phi_2 - \phi_2^{\rm sym}\right)$$

$$\bar{\Pi}^{08}(\phi_2, \phi_4) = \lambda_1\left(\phi_4 - 3/2\phi_2\right)$$

$$\bar{\Pi}^{i=33,88}(a^2/8t_0^{\rm sym}, \phi_2, \phi_4) = \bar{\Pi}^{\rm sym} + \gamma_1^i\left(\phi_2 - \phi_2^{\rm sym}\right) + \eta_1\left(\phi_4 - \phi_4^{\rm sym}\right)$$

$$+ \gamma_2^i \begin{cases} \log\left(\phi_2/\phi_2^{\rm sym}\right) \\ \left(\phi_2 - \phi_2^{\rm sym}\right)^2 \end{cases} + \begin{cases} \delta_2^d\left(a^2/8t_0^{\rm sym}\right) \\ \delta_2^d\left(a^2/8t_0^{\rm sym}\right) + \delta_3^d\left(a^2/8t_0^{\rm sym}\right)^{3/2} \end{cases}$$

Total least-squares minimisation

We employ the *least_squares* routine of the SciPy package [Virtanen et al. 2020], which uses the Levenberg-Marquardt algorithm [Ranganathan 2004].
Different ensembles are uncorrelated,

$$\chi^2 = \sum_e \chi_e^2 \equiv \sum_e \begin{cases} \chi^2_{e,-}, & \text{if } M_{\pi,e} \neq M_{K,e}, \\ 1/2\left(\chi^2_{e,33} + \chi^2_{e,88}\right), & \text{if } M_{\pi,e} = M_{K,e}. \end{cases}$$

The index e runs over the ensembles.
$\chi^2_{e,-}$, $\chi^2_{e,33}$ and $\chi^2_{e,88}$ can be written with the same generic structure $r^T \mathrm{Cov}^{-1} r$, where

$r = \text{model} - \text{data}$ is the vector of residues.

Cov is the covariance matrix, whose entries can be computed using

$$\mathrm{Cov}_{e,\cdot}[x, y] = \frac{1}{N_b - 1} \sum_{s=1}^{N_b} (x_s - E[x])\,(y_s - E[y])\,,$$

where s runs over the bootstrap samples, of which there are N_b in total.

r and Cov for non-SU(3)$_f$-symmetric ensembles

The residue vector is defined as

$$r_{e,-} = \begin{pmatrix} \phi_2 \\ \phi_4 \\ \bar{\Pi}(a, \phi_2, \phi_4; d = \mathrm{l}, i = 33) \\ \bar{\Pi}(a, \phi_2, \phi_4; d = \mathrm{s}, i = 33) \\ \bar{\Pi}(a, \phi_2, \phi_4; d = \mathrm{l}, i = 88) \\ \bar{\Pi}(a, \phi_2, \phi_4; d = \mathrm{s}, i = 88) \end{pmatrix} - \begin{pmatrix} \phi_2 \\ \phi_4 \\ \bar{\Pi}^{\mathrm{l}}_{33} \\ \bar{\Pi}^{\mathrm{s}}_{33} \\ \bar{\Pi}^{\mathrm{l}}_{88} \\ \bar{\Pi}^{\mathrm{s}}_{88} \end{pmatrix}_e ,$$

where e runs over the ensembles data. The index structure of the covariance matrix is

$$\mathrm{Cov}_{e,-} = \begin{pmatrix} \phi_2, \phi_2 & \phi_2, \phi_4 & \phi_2, \bar{\Pi}^{\mathrm{l}}_{33} & \phi_2, \bar{\Pi}^{\mathrm{s}}_{33} & \phi_2, \bar{\Pi}^{\mathrm{l}}_{88} & \phi_2, \bar{\Pi}^{\mathrm{s}}_{88} \\ \vdots & \phi_4, \phi_4 & \phi_4, \bar{\Pi}^{\mathrm{l}}_{33} & \phi_4, \bar{\Pi}^{\mathrm{s}}_{33} & \phi_4, \bar{\Pi}^{\mathrm{l}}_{88} & \phi_4, \bar{\Pi}^{\mathrm{s}}_{88} \\ \vdots & \vdots & \bar{\Pi}^{\mathrm{l}}_{33}, \bar{\Pi}^{\mathrm{l}}_{33} & \bar{\Pi}^{\mathrm{l}}_{33}, \bar{\Pi}^{\mathrm{s}}_{33} & \bar{\Pi}^{\mathrm{l}}_{33}, \bar{\Pi}^{\mathrm{l}}_{88} & \bar{\Pi}^{\mathrm{l}}_{33}, \bar{\Pi}^{\mathrm{s}}_{88} \\ \vdots & \vdots & \vdots & \bar{\Pi}^{\mathrm{s}}_{33}, \bar{\Pi}^{\mathrm{s}}_{33} & \bar{\Pi}^{\mathrm{s}}_{33}, \bar{\Pi}^{\mathrm{l}}_{88} & \bar{\Pi}^{\mathrm{s}}_{33}, \bar{\Pi}^{\mathrm{s}}_{88} \\ \vdots & \vdots & \vdots & \vdots & \bar{\Pi}^{\mathrm{l}}_{88}, \bar{\Pi}^{\mathrm{l}}_{88} & \bar{\Pi}^{\mathrm{l}}_{88}, \bar{\Pi}^{\mathrm{s}}_{88} \\ \cdots & \cdots & \cdots & \cdots & \cdots & \bar{\Pi}^{\mathrm{s}}_{88}, \bar{\Pi}^{\mathrm{s}}_{88} \end{pmatrix}_e$$

r and Cov for $\mathrm{SU}(3)_f$-symmetric ensembles

The residue vector is defined as

$$r_{e,i} = \begin{pmatrix} \phi_2 \\ \bar{\Pi}(a, \phi_2, 3\phi_2/2; d = \mathrm{l}, i) \\ \bar{\Pi}(a, \phi_2, 3\phi_2/2; d = \mathrm{s}, i) \end{pmatrix} - \begin{pmatrix} \phi_2 \\ \bar{\Pi}_i^{\mathrm{l}} \\ \bar{\Pi}_i^{\mathrm{s}} \end{pmatrix}_e ,$$

where e runs over the ensembles data. The index structure of the covariance matrix is

$$\mathrm{Cov}_{e,i} = \begin{pmatrix} \phi_2, \phi_2 & \phi_2, \bar{\Pi}_i^{\mathrm{l}} & \phi_2, \bar{\Pi}_i^{\mathrm{s}} \\ \vdots & \bar{\Pi}_i^{\mathrm{l}}, \bar{\Pi}_i^{\mathrm{l}} & \bar{\Pi}_i^{\mathrm{l}}, \bar{\Pi}_i^{\mathrm{s}} \\ \dots & \dots & \bar{\Pi}_i^{\mathrm{s}}, \bar{\Pi}_i^{\mathrm{s}} \end{pmatrix}_e$$

Jacobian

We define a vector y of length $m \times 1$ containing all the fit parameters,

$$y \equiv (\bar{\Pi}^{\text{sym}},\ \alpha_{2,\text{S}},\ \alpha_{3,\text{S}},\ \beta_{1,33},\ \text{etc.})$$

The vector y includes ϕ_2 for the $\text{SU}(3)_f$-symmetric ensembles, and ϕ_2 and ϕ_4 for the rest.
Then, we apply the Cholesky decomposition on $\chi^2_{e,-}$, $\chi^2_{e,33}$, χ^2_{88},

$$\chi_{e,\cdot} = L^{-1}_{e,\cdot} r_{e,\cdot},$$

such that $\chi_{e,\cdot}$ is a $n \times 1$ vector, with n the number of dependent ($\bar{\Pi}$) plus independent (ϕ_2, ϕ_4) variables for a given ensemble.
Then, we compute the $m \times n$ matrix of derivatives

$$\left(\frac{\partial \chi_{e,\cdot}}{\partial y}\right)^T = L^{-1}_{e,\cdot}\left(\frac{\partial r_{e,\cdot}}{\partial y}\right)^T,$$

For $\text{SU}(3)_f$-symmetric ensembles, $m = 10$ and $n = 3$, while $m = 11$ and $n = 6$ for the rest. Then, the Jacobian for every ensemble is [Turkington 2013]

$$\frac{\partial \chi_e}{\partial y}\chi_e = \begin{cases} \frac{\partial \chi_{e,-}}{\partial y}\chi_{e,-}, & \text{if } M_{\pi,e} \neq M_{K,e} \\ \frac{1}{2}\left(\frac{\partial \chi_{e,\mathbf{33}}}{\partial y}\chi_{e,33} + \frac{\partial \chi_{e,\mathbf{88}}}{\partial y}\chi_{e,88}\right), & \text{if } M_{\pi,e} = M_{K,e}. \end{cases}$$

Lattice spacing dependence

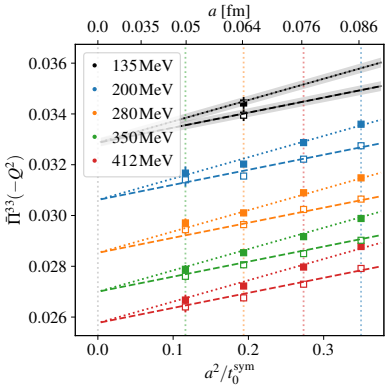

Logarithmic corrections to the a^2 behaviour

[Cè et al. 2021]

$$\tilde{c}_{\bar{\Pi}}(Q^2)\cdot(a^2/t_0^{\rm sym})\log\left(t_0^{\rm sym}/a^2\right)/2 \to 0$$

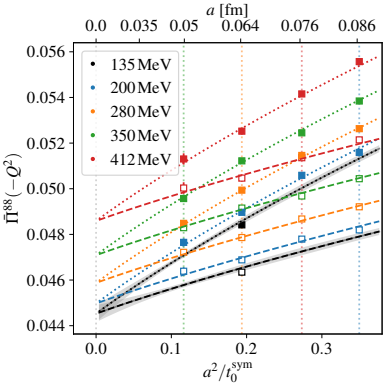

Step function to transition between a^2 and $a^2 + a^3$

$$\Theta(Q^2) = 0.5\left(1 + \tanh\left((Q^2 - 2.5\,\text{GeV}^2)/1.0\,\text{GeV}^2\right)\right)$$

Relating $\bar{\Pi}$ and the Stieltjes function

The integral representation of a Stieltjes function $\Phi(z)$ is [Hadamard 1892; Aubin et al. 2012],

$$\Phi(z) = \int_0^{1/R} \frac{\mathrm{d}\nu(\tau)}{1+\tau z},$$

where $\nu(z)$ is real, bounded, non-decreasing on the interval $[0, 1/R]$, and takes infinitely many values on that said interval. $\Phi(z)$ is analytic in the entire complex plane except on the cut $z \in (-\infty, -R]$, and decreases monotonically in the range $z \in (-R, \infty)$.Choosing [Aubin et al. 2012]

$$\tau = \frac{1}{s}, \qquad \mathrm{d}\nu(\tau) = \mathrm{d}\tau\ \rho(1/\tau),$$

$$R = 4M_\pi^2, \qquad \rho(1/\tau) = \frac{1}{\pi}\mathrm{Im}\Pi(1/\tau),$$

we see that $\bar{\Pi}$ is a Stieltjes function [Aubin et al. 2012],

$$\bar{\Pi}(Q^2) = Q^2\Phi(Q^2), \qquad \Phi(Q^2) = \int_{4M_\pi^2}^{\infty} \mathrm{d}s\ \frac{\rho(s)}{s(s+Q^2)}.$$

The spectral function $\rho(s)$ is non-negative in the integration range.

Relating the Stieltjes function and the Padé approximants (PAs)

A acro:padePadé approximant (PA) $R_M^N(Q^2)$ is the ratio of two polynomials of degrees N and M [Barnsley 1973],

$$R_M^N(Q^2) = \frac{\sum_{n=0}^{N} a_n Q^{2n}}{1 + \sum_{m=1}^{M} b_m Q^{2m}}$$

To build PAs to describe $\Phi(Q^2)$, we employ the following theorem [Barnsley 1973; George A. Baker 1969]: Given P points $(Q_i^2, \Phi(Q_i^2))$, $i \in \{1, \ldots, \mathrm{P}\}$, a sequence of Padé approximants can be constructed converging to $\Phi(Q^2)$ in the limit $\mathrm{P} \to \infty$ on any closed, bounded region of the complex plane, excluding the cut $Q^2 \in (-\infty, -4M_\pi^2]$. Then, the Stieltjes function $\Phi(Q^2)$ can be built as a continued fraction [Barnsley 1973],

$$\Phi(Q^2) = \cfrac{\psi_1(Q_1^2)}{1 + \cfrac{(Q^2 - Q_1^2)\,\psi_2(Q_2^2)}{1 + \cfrac{(Q^2 - Q_2^2)\,\psi_3(Q_3^2)}{\ddots\, 1 + (Q^2 - Q_{\mathrm{P}-1}^2)\,\psi_{\mathrm{P}}(Q_{\mathrm{P}}^2)}}}.$$

The functions ψ_i can be constructed recursively using [G. A. Baker 1969]

$$\psi_1 = \Phi(Q_1^2), \qquad \psi_i(Q^2) = \frac{\psi_{i-1}(Q_{i-1}^2) - \psi_{i-1}(Q_i^2)}{(Q^2 - Q_{i-1}^2)\psi_{i-1}(Q^2)}, \qquad i > 1.$$

Euclidean split technique

To compute $\alpha(q^2)$ and avoid using e^+e^--data, we need to connect the LQCD determination in the space-like region $Q^2 = -q^2 > 0$ with the time-like energy $q^2 > 0$.
We do this via the Adler function [Adler 1974],

$$D(Q^2) = \frac{3\pi}{\alpha} Q^2 \frac{\mathrm{d}(\Delta\alpha)_{\mathrm{had}}(Q^2)}{\mathrm{d}Q^2}$$

Upon integration [Jegerlehner 1999]

$$(\Delta\alpha)^{(5)}_{\mathrm{had}}(M_Z^2) = (\Delta\alpha)^{(5)}_{\mathrm{had}}(Q_0^2) + \left[(\Delta\alpha)^{(5)}_{\mathrm{had}}(-M_Z^2) - (\Delta\alpha)^{(5)}_{\mathrm{had}}(Q_0^2)\right]^{\mathrm{pQCD}} + \left[(\Delta\alpha)^{(5)}_{\mathrm{had}}(M_Z^2) - (\Delta\alpha)^{(5)}_{\mathrm{had}}(-M_Z^2)\right]^{\mathrm{pQCD}}$$

Q_0^2 must be large enough to apply pQCD, but also small enough to be computed on the lattice

Particular values of α

$$(\Delta\alpha)_{\text{lep}}(M_Z^2) = 314.979(2) \times 10^{-4} \quad \text{[Sturm 2013; Steinhauser 1998]},$$

$$(\Delta\alpha)_{\text{had}}^{(5)}(M_Z^2) = 276.09(112) \times 10^{-4} \quad \text{[Keshavarzi, Nomura, and Teubner 2020]},$$

$$(\Delta\alpha)_t(M_Z^2) = -0.7201(37) \times 10^{-4} \text{[Keshavarzi, Nomura, and Teubner 2020]}.$$